Production of Λ^0, $\overline{\Lambda}^0$, $\Xi^\pm$, and $\Omega^\pm$ Hyperons in $p\overline{p}$ Collisions at $\sqrt{s} = 1.96$ TeV

T. Aaltonen, E. Brucken, F. Devoto, P. Mehtala, and R. Orava

Division of High Energy Physics, Department of Physics,

University of Helsinki and Helsinki Institute of Physics, FIN-00014, Helsinki, Finland

B. Álvarez González[v], B. Casal, J. Cuevas[v], G. Gomez, E. Palencia[f],

T. Rodrigo, A. Ruiz, L. Scodellaro, I. Vila, and R. Vilar

Instituto de Fisica de Cantabria, CSIC-University of Cantabria, 39005 Santander, Spain

S. Amerio, M. Bauce[cc], D. Bisello[cc], G. Busetto[cc], G. Compostella[cc], M. d'Errico[cc],

T. Dorigo, A. Gresele, I. Lazzizzera, D. Lucchesi[cc], and S. Pagan Griso[cc]

Istituto Nazionale di Fisica Nucleare, Sezione di Padova-Trento,

[cc] *University of Padova, I-35131 Padova, Italy*

D. Amidei, M. Campbell, A. Eppig, D. Mietlicki,

G.L. Strycker, M. Tecchio, A. Varganov, and T. Wright

University of Michigan, Ann Arbor, Michigan 48109, USA

A. Anastassov, M. Schmitt, and D. Stentz

Northwestern University, Evanston, Illinois 60208, USA

A. Annovi, M. Cordelli, P. Giromini, F. Happacher, M.J. Kim, F. Ptohos[h], and S. Torre

Laboratori Nazionali di Frascati, Istituto Nazionale

di Fisica Nucleare, I-00044 Frascati, Italy

J. Antos, P. Bartos, A. Brisuda, R. Lysak, and S. Tokar

Comenius University, 842 48 Bratislava,

Slovakia; Institute of Experimental Physics, 040 01 Kosice, Slovakia

G. Apollinari, J.A. Appel, W. Ashmanskas, W. Badgett, A. Beretvas, M. Binkley*,

B. Brau[a], K. Burkett, F. Canelli[12], S. Carron, M. Casarsa, P. Catastini, G. Chlachidze,

F. Chlebana, M.E. Convery, R. Culbertson, D. Dagenhart, M. Datta, P. Dong,

* Deceased

J.C. Freeman, E. Gerchtein, C.M. Ginsburg, D. Glenzinski, A. Golossanov,
R.C. Group, S.R. Hahn, A. Hocker, W. Hopkins[g], E. James, S. Jindariani, T.R. Junk,
B. Kilminster, S. Lammel, J.D. Lewis, M. Lindgren, D.O. Litvintsev, T. Liu,
P. Lukens, R. Madrak, K. Maeshima, T. Miao, M.N. Mondragon[k], R. Moore,
M.J. Morello, P. Movilla Fernandez, A. Mukherjee, P. Murat, J. Nachtman[m],
V. Papadimitriou, J. Patrick, A. Pronko, L. Ristori[45], R. Roser, V. Rusu, P. Schlabach,
E.E. Schmidt, F.D. Snider, A. Soha, P. Squillacioti, J. Thom[g], S. Tkaczyk, D. Tonelli,
D. Torretta, G. Velev, R.L. Wagner, W.C. Wester III, E. Wicklund, P. Wilson,
P. Wittich[g], S. Wolbers, G.P. Yeh, K. Yi[m], J. Yoh, S.S. Yu, and J.C. Yun
Fermi National Accelerator Laboratory, Batavia, Illinois 60510, USA

A. Apresyan, V.E. Barnes, D. Bortoletto, G. Flanagan[r], A.F. Garfinkel, M. Jones,
A.T. Laasanen, Q. Liu, F. Margaroli, K. Potamianos, N. Ranjan, and A. Sedov
Purdue University, West Lafayette, Indiana 47907, USA

T. Arisawa, K. Ebina, N. Kimura, K. Kondo, J. Naganoma, and K. Yorita
Waseda University, Tokyo 169, Japan

A. Artikov, J. Budagov, D. Chokheli, V. Glagolev, O. Poukhov*,
F. Prokoshin[y], A. Semenov, A. Simonenko, A. Sissakian*, and I. Suslov
Joint Institute for Nuclear Research, RU-141980 Dubna, Russia

J. Asaadi, A. Aurisano, A. Elagin, R. Eusebi, D. Goldin, T. Kamon, V. Khotilovich,
V. Krutelyov[d], E. Lee, S.W. Lee[w], P. McIntyre, A. Safonov, D. Toback, and M. Weinberger
Texas A&M University, College Station, Texas 77843, USA

B. Auerbach, C. Cuenca Almenar, U. Husemann,
S. Lockwitz, A. Loginov, M.P. Schmidt*, and M. Stanitzki
Yale University, New Haven, Connecticut 06520, USA

F. Azfar, S. Farrington, C. Hays, J. Linacre, L. Oakes, and P. Renton
University of Oxford, Oxford OX1 3RH, United Kingdom

A. Barbaro-Galtieri, A. Cerri[f], H.C. Fang, C. Haber,

C.-J. Lin, P. Lujan, J. Lys, J. Nielsen[e], and W.-M. Yao
Ernest Orlando Lawrence Berkeley National Laboratory, Berkeley, California 94720, USA

B.A. Barnett, S. Behari, B. Blumenfeld, G. Giurgiu, P. Maksimovic, and M. Mathis
The Johns Hopkins University, Baltimore, Maryland 21218, USA

P. Barria[ee], F. Bedeschi, G. Bellettini[dd], M. Bucciantonio[dd], R. Carosi,
V. Cavaliere[ee], G. Chiarelli, M.A. Ciocci[ee], F. Crescioli[dd], M. Dell'Orso[dd],
A. Di Canto[dd], B. Di Ruzza, S. Donati[dd], C. Ferrazza[ff], P. Garosi[ee],
P. Giannetti, M. Giunta, G. Introzzi, S. Lami, G. Latino[ee], S. Leo[dd], S. Leone,
A. Menzione, G. Piacentino, G. Punzi[dd], F. Ruffini[ee], L. Sartori, A. Scribano[ee],
F. Scuri, F. Sforza[dd], M. Trovato[ff], N. Turini[ee], E. Vataga[ff], and G. Volpi[dd]
Istituto Nazionale di Fisica Nucleare Pisa, [dd] University of Pisa,
[ee] University of Siena and [ff] Scuola Normale Superiore, I-56127 Pisa, Italy

G. Bauer, G. Gomez-Ceballos, M. Goncharov, K. Makhoul, and C. Paus
Massachusetts Institute of Technology,
Cambridge, Massachusetts 02139, USA

D. Beecher, I. Bizjak[ii], L. Cerrito[q], M. Lancaster, E. Nurse, and D. Waters
University College London, London WC1E 6BT, United Kingdom

J. Bellinger, D. Carlsmith, W.H. Chung, M. Herndon,
J. Nett, L. Pondrom, J. Pursley, and V. Ramakrishnan
University of Wisconsin, Madison, Wisconsin 53706, USA

D. Benjamin, A. Bocci, S. Cabrera[x], J. Deng[c], A.T. Goshaw, B. Jayatilaka, A.V. Kotwal,
M. Kruse, S.H. Oh, T.J. Phillips, C. Wang, A. Wen, J. Yamaoka, G.B. Yu, and Y. Zeng
Duke University, Durham, North Carolina 27708, USA

A. Bhatti, L. Demortier, M. Gallinaro, K. Goulianos, G. Lungu, S. Malik, and C. Mesropian
The Rockefeller University, New York, New York 10065, USA

K.R. Bland, J.R. Dittmann, M.J. Frank, K. Hatakeyama,

S. Hewamanage, N. Krumnack[l], and Z. Wu
Baylor University, Waco, Texas 76798, USA

C. Blocker and D. Clark
Brandeis University, Waltham, Massachusetts 02254, USA

A. Bodek, H.S. Budd, Y.S. Chung, P. de Barbaro,
J.Y. Han, K.S. McFarland, and W.K. Sakumoto
University of Rochester, Rochester, New York 14627, USA

J. Boudreau, K. Gibson, C. Liu, A. Rahaman, and P.F. Shepard
University of Pittsburgh, Pittsburgh, Pennsylvania 15260, USA

A. Boveia, C. Grosso-Pilcher, M. Hurwitz, W. Ketchum, Y.K. Kim, D. Krop,
S. Kwang, H.S. Lee, S. Shiraishi, M. Shochet, J. Tang, S. Wilbur, and U.K. Yang[p]
Enrico Fermi Institute, University of Chicago, Chicago, Illinois 60637, USA

L. Brigliadori[bb], A. Castro[bb], M. Deninno, M.K. Jha, P. Mazzanti,
N. Moggi, M. Mussini[bb], F. Rimondi[bb], and S. Zucchelli[bb]
Istituto Nazionale di Fisica Nucleare Bologna,
[bb] *University of Bologna, I-40127 Bologna, Italy*

C. Bromberg, M. Campanelli, Z. Gunay-Unalan, M. Hussein, J. Huston, and K. Tollefson
Michigan State University, East Lansing, Michigan 48824, USA

S. Budd, B. Carls, D. Errede, S. Errede, H. Gerberich, M.S. Neubauer,
O. Norniella, K. Pitts, E. Rogers, A. Sfyrla, and G.A. Thompson
University of Illinois, Urbana, Illinois 61801, USA

P. Bussey, A. Robson, and R. St. Denis
Glasgow University, Glasgow G12 8QQ, United Kingdom

A. Buzatu, N. Hussain, P. Sinervo, B. Stelzer, O. Stelzer-Chilton, and A. Warburton
Institute of Particle Physics: McGill University, Montréal,
Québec, Canada H3A 2T8; Simon Fraser University, Burnaby,

British Columbia, Canada V5A 1S6; University of Toronto,
Toronto, Ontario, Canada M5S 1A7; and TRIUMF,
Vancouver, British Columbia, Canada V6T 2A3

C. Calancha, J.P. Fernandez, O. González, R. Martínez-Ballarín,
I. Redondo, P. Ttito-Guzmán, and M. Vidal
Centro de Investigaciones Energeticas Medioambientales
y Tecnologicas, E-28040 Madrid, Spain

S. Camarda, M. Cavalli-Sforza, G. De Lorenzo, C. Deluca,
S. Grinstein, M. Martínez, L. Ortolan, and V. Sorin
Institut de Fisica d'Altes Energies, Universitat Autonoma de Barcelona,
E-08193, Bellaterra (Barcelona), Spain

A. Canepa, J. Heinrich, J. Keung, J. Kroll, E. Lipeles, N.S. Lockyer, C. Neu[z], E. Pianori,
T. Rodriguez, E. Thomson, Y. Tu, P. Wagner, D. Whiteson[c], and H.H. Williams
University of Pennsylvania, Philadelphia, Pennsylvania 19104, USA

S. Carrillo[k], R. Field, I. Furic, N. Goldschmidt, S. Klimenko,
J. Konigsberg, A. Korytov, I. Oksuzian, A. Sukhanov, and F. Vázquez[k]
University of Florida, Gainesville, Florida 32611, USA

D. Cauz, C. Pagliarone, G. Pauletta[hh], A. Penzo,
M. Rossi, L. Santi[hh], P. Totaro[hh], and A. Zanetti
Istituto Nazionale di Fisica Nucleare Trieste/Udine,
I-34100 Trieste, [hh] University of Trieste/Udine, I-33100 Udine, Italy

Y.C. Chen, S. Hou, A. Mitra, P.K. Teng, and S.M. Wang
Institute of Physics, Academia Sinica,
Taipei, Taiwan 11529, Republic of China

M. Chertok, J. Conway, C.A. Cox, D.J. Cox, R. Erbacher, R. Forrest, A. Ivanov[o],
W. Johnson, R.L. Lander, D.E. Pellett, T. Schwarz, S.Z. Shalhout, and J.R. Smith
University of California, Davis, Davis, California 95616, USA

K. Cho, E.J. Jeon, K.K. Joo, D.H. Kim, H.S. Kim, H.W. Kim, J.E. Kim, S.B. Kim,
D.J. Kong, J.S. Lee, C.S. Moon, Y.D. Oh, S. Uozumi, Y.C. Yang, and I. Yu
Center for High Energy Physics: Kyungpook National University,
Daegu 702-701, Korea; Seoul National University, Seoul 151-742,
Korea; Sungkyunkwan University, Suwon 440-746,
Korea; Korea Institute of Science and Technology Information,
Daejeon 305-806, Korea; Chonnam National University, Gwangju 500-757,
Korea; Chonbuk National University, Jeonju 561-756, Korea

J.P. Chou, M. Franklin, J. Guimaraes da Costa, and S. Moed
Harvard University, Cambridge, Massachusetts 02138, USA

C.I. Ciobanu, M.Corbo, N. d'Ascenzo[t], N. Ershaidat[aa], V. Saveliev[t], and A. Savoy-Navarro
LPNHE, Universite Pierre et Marie Curie/IN2P3-CNRS, UMR7585, Paris, F-75252 France

A. Clark, J.E. Garcia, A. Lister, and X. Wu
University of Geneva, CH-1211 Geneva 4, Switzerland

S. De Cecco, S. Giagu[gg], M. Iori[gg], P. Mastrandrea, and M. Rescigno
Istituto Nazionale di Fisica Nucleare, Sezione di Roma 1,
[gg]Sapienza Università di Roma, I-00185 Roma, Italy

M. D'Onofrio, G. Manca[b], R. McNulty[i], A. Mehta, and T. Shears
University of Liverpool, Liverpool L69 7ZE, United Kingdom

M. Feindt, M. Heck, D. Horn, M. Kreps, T. Kuhr, J. Lueck,
C. Marino, J. Morlock, Th. Muller, A. Schmidt, and F. Wick
Institut für Experimentelle Kernphysik,
Karlsruhe Institute of Technology, D-76131 Karlsruhe, Germany

J. Galyardt, D. Jang, S.Y. Jun, M. Paulini, E. Pueschel, J. Russ, and J. Thome
Carnegie Mellon University, Pittsburgh, Pennsylvania 15213, USA

V. Giakoumopoulou, N. Giokaris, A. Manousakis-Katsikakis, and C. Vellidis

University of Athens, 157 71 Athens, Greece

M. Gold, I. Gorelov, S. Seidel, J. Strologas, and M. Vogel
University of New Mexico, Albuquerque, New Mexico 87131, USA

E. Halkiadakis, D. Hare, D. Hidas, A. Lath, and S. Somalwar
Rutgers University, Piscataway, New Jersey 08855, USA

A. Hamaguchi, Y. Kato[n], T. Okusawa, Y. Seiya,
T. Wakisaka, K. Yamamoto, and T. Yoshida[j]
Osaka City University, Osaka 588, Japan

K. Hara, S.H. Kim, M. Kurata, H. Miyake, Y. Nagai, K. Sato, M. Shimojima[s],
Y. Sudo, K. Takemasa, Y. Takeuchi, T. Tomura, and F. Ukegawa
University of Tsukuba, Tsukuba, Ibaraki 305, Japan

M. Hare, A. Napier, S. Rolli, K. Sliwa, and B. Whitehouse
Tufts University, Medford, Massachusetts 02155, USA

R.F. Harr, P.E. Karchin, and M.E. Mattson
Wayne State University, Detroit, Michigan 48201, USA

R.E. Hughes, K. Lannon[u], J. Pilot, J.S. Wilson, B.L. Winer, and H. Wolfe
The Ohio State University, Columbus, Ohio 43210, USA

T. LeCompte, L. Nodulman, A.A. Paramonov, and A.B. Wicklund
Argonne National Laboratory, Argonne, Illinois 60439, USA

I. Nakano
Okayama University, Okayama 700-8530, Japan

C. Plager and R. Wallny
University of California, Los Angeles,
Los Angeles, California 90024, USA

I. Shreyber

[1] *Institution for Theoretical and Experimental Physics, ITEP, Moscow 117259, Russia*

[2] (Dated: January 18, 2011)

Abstract

We report a set of measurements of inclusive invariant p_T differential cross sections of Λ^0, $\overline{\Lambda}^0$, $\Xi^{\pm}$, and $\Omega^{\pm}$ hyperons reconstructed in the central region with pseudorapidity $|\eta| < 1$ and p_T up to 10 GeV/c. Events are collected with a minimum-bias trigger in $p\bar{p}$ collisions at a center-of-mass energy of 1.96 TeV using the CDF II detector at the Tevatron Collider. As p_T increases, the slopes of the differential cross sections are similar not only to each other but also to those of mesons, which could indicate a universality of the particle production in p_T The invariant differential cross sections are also presented for different charged-particle multiplicity intervals.

Ever since their discovery in cosmic ray interactions [1], particles containing strange quarks have been extensively studied at particle colliders (e^+e^- [2], ep [3], $p\bar{p}$ [4, 5] and pp [6]). The process by which hadrons in general are produced from interactions is an unsolved problem in the standard model, and a detailed analysis of production properties of particles with different quark flavors and numbers of quarks could pave the way to understanding the process from first principles. The data on strange particle production can also be used to refine phenomenological models and set parameters, such as the strange quark suppression constant in event generators, which have become an integral part of any data analysis. Interest in particles containing strange quarks increased with the introduction of the quark-gluon plasma (QGP). Formation of quark-gluon plasma in a collision could manifest itself as an enhanced production of strange particles such as kaons and hyperons [7]. To isolate QGP signatures in heavy-ion collision data, understanding the particle production properties from simple nucleon interactions is necessary.

There are ample data on the production of particles with one strange quark, but very little available on particles with two or more [8, 9]. Previous studies of hyperons from colliders such as RHIC [10], $Sp\overline{p}S$ [11], and the Tevatron [12, 13] were limited by low sample statistics and the limited accessible range of hyperon momentum component transverse to the beam direction (p_T). In this Letter, we report on a study of the hyperons Λ^0 (quark content uds), Ξ^- (dss), and Ω^- (sss) and their corresponding antiparticles ($\overline{\Lambda}^0$, Ξ^+, and Ω^+). For these hyperons, the inclusive invariant p_T differential cross sections are measured up to p_T of 10 GeV/c, based on $\sim$ 100 million minimum-bias events collected with the CDF II detector. The measurements reported here are the current best from any hadron collider experiment in terms of statistics and p_T range.

The CDF II detector is described in detail elsewhere [14]. The components most relevant to this analysis are those that comprise the tracking system, which is within a uniform axial magnetic field of 1.4T. The inner tracking volume is composed of a system of eight layers of silicon microstrip detectors ranging in radius from 1.5 to 28.0 cm [15] in the pseudorapidity region $|\eta| < 2$ [16]. The remainder of the tracking volume is occupied by the Central Outer Tracker (COT). The COT is a cylindrical drift chamber containing 96 sense-wire layers grouped in eight alternating superlayers of axial and stereo wires [17]. Its active volume covers 40 to 140 cm in radius and $|z| < 155$ cm. The transverse-momentum resolution of tracks reconstructed using COT hits is $\sigma(p_T)/p_T^2 \sim 0.0017/(\mathrm{GeV}/c)$.

Events for this analysis are collected with a "minimum-bias" (MB) trigger, which selects beam crossings with at least one $p\bar{p}$ interaction by requiring a timing coincidence for signals in both forward and backward gas Cherenkov counters [18] covering the regions $3.7 < |\eta| < 4.7$. The MB trigger is rate-limited to keep the final trigger output at 1 Hz. Primary event vertices are identified by the convergence of reconstructed tracks along the beam axis. Events are accepted that contain a reconstructed vertex in the fiducial region $|z_{vtx}| \leq 60$ cm centered around the nominal CDF origin ($z = 0$). When an event has more than one vertex, the highest quality vertex, usually the one with the most associated tracks, is selected and it is required that there be no other vertices within ± 5 cm of this vertex. This selection introduces a bias toward high multiplicity events as the instantaneous luminosity increases. To combine events collected at different average instantaneous luminosities, we determine a per-event weight as a function of the charged-track multiplicity N_{ch} in order to match the multiplicity distribution of a data sample where the average number of interactions is less than 0.3 per bunch crossing. For the N_{ch} calculation, tracks are required to have a high track-fit quality with χ^2 per degree-of-freedom (χ^2/dof) less than 2.5, and more than five hits in at least two axial and two stereo COT segments. It is further required that tracks satisfy $|\eta| < 1$, impact parameter d_0 [19] less than 0.25 cm, the distance along the z-axis (δZ_0)between the event vertex and the track position at the point of closest approach to the vertex in the $r - \phi$ plane be less than 2 cm, and $p_T > 0.3$ GeV/c. The p_T selection is to minimize the inefficiency of the track-finding algorithm for low momentum tracks.

We search for $\Lambda^0 \to p\pi^-$ decays using tracks with opposite-sign charge and $p_T > 0.325$ GeV/c that satisfy the χ^2/dof and COT segment requirements. In this Letter, any reference to a specific hyperon state implies the antiparticle state as well. For each two-track combination we calculate their intersection coordinate in the $r - \phi$ plane. Once this intersection point, referred to as the secondary vertex, is found, the z-coordinate of each track (Z_1 and Z_2) is calculated at that point. If the distance $|Z_1 - Z_2|$ is less than 1.5 cm, the tracks are considered to originate from a Λ^0 candidate decay. The pair is traced back to the vertex and we require δZ_0 be less than 2 cm, and the d_0 be less than 0.25 cm. To reduce backgrounds further, we require the Λ^0 decay length L_{Λ^0}, the distance in the $r - \phi$ plane between the primary and secondary vertices, to be greater than 2.5 cm and less than 50 cm.

The invariant mass $M_{p\pi}$ of the two-track system is calculated by attributing the proton mass to the track with the higher p_T, as preferentially expected by the kinematics of a Λ^0

decay. Figure 1 shows the invariant mass for Λ^0 candidates with $|\eta| < 1$. This distribution is divided into 23 p_T intervals [20] and the number of Λ^0 in each p_T interval is determined by fitting the invariant mass distributions using a Gaussian function with three parameters for the signal and a third-order polynomial for the underlying combinatorial background. The data in the mass range $1.10 - 1.16$ GeV/c^2 are fitted. The polynomial fit to the background is subtracted bin-by-bin from the data entries in the Λ^0 mass window ($1.111 - 1.121$ GeV/c^2) to obtain the number of Λ^0 hyperons. This number is divided by the acceptance to obtain the invariant p_T differential cross section as described later.

The fitting procedure is one source of systematic uncertainty. This uncertainty is estimated by separately varying the mass range of the fit, the functional form for the signal to a double Gaussian, and the background modeling function to a second-order polynomial. The number of Λ^0 is recalculated in all p_T intervals for each variation. The systematic uncertainty is determined as the sum in quadrature of the fractional change in the number of Λ^0 from each modified fit. It decreases from $\pm 10\%$ at the lowest p_T (1.2 GeV/c) to less than $\pm 5\%$ for $p_T > 1.75$ GeV/c.

The cascade reconstruction decay mode is $\Xi^- \to \Lambda^0\pi^- \to (p\pi^-)\pi^-$. The previously reconstructed Λ^0 candidates are used, but without the d_0 and δZ_0 requirements. We select Λ^0 candidates in the Λ^0 mass window and calculate the coordinate of the intersection point in the $r - \phi$ plane between the Λ^0 candidate and a third track. The z-axis coordinates at this point are calculated for the third track (Z_3) and the Λ^0 candidate (Z_4). The three-track system is considered a Ξ^- candidate decay if the distance $|Z_3 - Z_4| < 1.5$ cm. We also require the decay length $L_{\Xi^-} > 1$ cm, and $(L_{\Lambda^0} - L_{\Xi^-}) > 1$ cm. Finally, it is required that the d_0 and δZ_0 of the Ξ^- candidate be less than 0.25 cm and 2 cm respectively.

The invariant mass $M_{\Lambda^0\pi}$ is calculated by fixing the mass of the Λ^0 candidate to 1.1157 GeV/c^2 [21] and assigning the pion mass to the third track. Figure 1 shows the invariant mass for Ξ^- candidates with $|\eta| < 1$.

The Ξ^- candidates are divided into 17 p_T intervals and the number of Ξ^- in each interval is determined by fitting the corresponding $M_{\Lambda^0\pi}$ invariant mass distribution using a Gaussian function for the signal and a third-order polynomial for the background. The fitted background is then subtracted bin-by-bin from the data entries in the signal region (1.31 to 1.33 GeV/c^2) to obtain the Ξ^- yield in every p_T interval. The systematic uncertainty of the fit procedure is estimated the same way as for the Λ^0 and is found to change by no more

than $\pm 5\%$ in all p_T intervals.

To reconstruct Ω^- decays we follow the same procedure as for the Ξ^- and apply the same selection criteria except that the third track is assigned the kaon mass. The search decay mode is $\Omega^- \to \Lambda^0 K^- \to (p\pi^-)K^-$. Because of the larger background, the procedure to extract the Ω^- signal yield is slightly different from that in the previous cases. Track pairs with $M_{p\pi^-}$ in the mass ranges $1.095 - 1.105$ and $1.127 - 1.137$ GeV/c^2 are combined with the third track to obtain the invariant mass distribution of the combinatorial background. This distribution is subtracted from the $M_{\Lambda^0 K^-}$ distribution after normalizing to the number of events in the mass window $1.69 < M_{\Lambda^0 K^-} < 1.74$ GeV/c^2. The background subtracted $M_{\Lambda^0 K^-}$ invariant mass distribution is shown in Fig. 1.

The distribution is divided into 10 p_T intervals, and we use the method described above to extract the Ω^- signal from the corresponding invariant mass distributions in each p_T interval within the mass window 1.66 to 1.68 GeV/c^2. The systematic uncertainty due to the fitting procedure is also calculated in a similar manner as Ξ^-, with the exception of using a double Gaussian variation because of low Ω^- statistics. The overall uncertainties are about $\pm 10\%$ for all p_T intervals.

The geometric and kinematic acceptance is estimated with Monte Carlo (MC) simulations. The MC data of a resonance state are generated with fixed p_T corresponding to 14 points [20] ranging from 0.75 to 10 GeV/c and flat in rapidity $|y| < 2$. A generated resonance is combined with either one or four non-diffractive inelastic MB events generated with the PYTHIA [22] generator. Although the average number of interactions in our data sample is a little less than two, the default acceptance is calculated from the MC sample with four MB events and the difference of the acceptance values between the two samples is one of our systematic uncertainties. Based on a study with tracks from K^0_S decay, the sample with four MB events reproduces the low p_T tracking efficiency in data well within the systematic uncertainty

The detector response to particles produced in the simulation is modeled with the CDF II detector simulation that in turn is based on the GEANT-3 MC program [23]. Simulated events are processed and selected with the same analysis code used for the data. The acceptance is defined as the ratio of the number of reconstructed resonances with the input p_T over the generated number, including the branching ratio. Acceptance values are calculated separately for the particles and their corresponding antiparticles and the average of the

two is used as the default value, since the acceptances for the two states are similar. The acceptance values obtained for the 14 p_T points are fitted with a fourth order polynomial function and the fitted curve is used to correct the numbers of each hyperon state in the data.

The modeling of the MB events overlapping with the examined resonance and the selection criteria applied contribute as a systematic uncertainty to the acceptance calculation. The contribution from the former has already been mentioned. Acceptance uncertainties due to the selection criteria are studied by changing the selection values of the variables used to reconstruct the resonances. The variables examined are p_T, $|Z_1 - Z_2|$, $|Z_3 - Z_4|$, δZ_0, d_0 and the decay lengths. For each variable other than p_T, two values around the default value are typically chosen. One value is such that it has little effect on the signal, and the other reduces the signal by ∼20 to 30%. The default p_T selection value is 0.325 GeV/c, and it is changed to 0.3 GeV/c and to 0.35 GeV/c.

For each considered variation, a new acceptance curve and the number of resonances as a function of p_T are obtained, and the percentage change between the new p_T distribution and the one with the default selection requirements is taken as the uncertainty in the acceptance for the specific p_T interval. The square root of the quadratic sum of the uncertainties from each variation is taken as the total conservative uncertainty on the acceptance in a given p_T bin. The systematic uncertainty associated with the Ω^- hyperon acceptance is derived from the Ξ^- uncertainty estimate since the reconstruction follows the same criteria. This acceptance uncertainty is added quadratically to the systematic uncertainty due to the fitting procedure, described earlier, to give the total systematic uncertainty.

For the Λ^0 case, the acceptance uncertainty decreases from about 25% at $p_T \sim 1$ GeV/c to 10% at $p_T \sim 2$ GeV/c and then rises again slowly to 15% for $p_T > 7$ GeV/c. The corresponding acceptance uncertainty for the Ξ^- (Ω^-) case decreases from about 15% (20%) at $p_T \sim 2$ GeV/c to 10% (15%) for $p_T > 4$ GeV/c.

The inclusive invariant p_T differential cross section for each hyperon resonance is calculated as $Ed^3\sigma/dp^3 = (\sigma_{mb}/N_{event})d^3N/Ap_T dp_T dy d\phi = (\sigma_{mb}/2\pi N_{event})\Delta N/Ap_T \Delta p_T \Delta y$ where σ_{mb} is our MB trigger cross section, N_{event} is the number of weighted events, ΔN is the number of hyperons observed in each p_T interval (Δp_T) after background subtraction, A is the acceptance in the specific p_T interval, and Δy is the rapidity range used in the acceptance calculation (-2 to 2).

TABLE I: The results of power law function fits to the p_T differential cross sections described in the text and shown in Fig. 2 for $p_T > 2$ GeV/c. The parameter p_0 is fixed to 1.3 GeV/c in all fits. The K^0_S values are from Ref. [25] at $\sqrt{s} = 1.8$ TeV. The uncertainties shown do not include the MB cross section uncertainty [24]. The last line of the table gives the χ^2 per degree-of-freedom of the fit to data.

Parameter (units)	K^0_S [25]	Λ^0	$\Xi^\pm$	$\Omega^\pm$
A (mb/GeV$^2c^3$)	45 ± 9	210 ± 25	14.9 ± 2.5	1.50 ± 0.75
p_0 (GeV/c)	1.3	1.3	1.3	1.3
n	7.7 ± 0.2	8.81 ± 0.08	8.26 ± 0.12	8.06 ± 0.34
χ^2/dof	8.1/11	5.7/15	15.8/15	10.5/7

Figure 2 shows the results for the p_T differential cross section for the three hyperon resonances. The uncertainties shown for each data point include the statistical and all systematic uncertainties described above, except the one associated with σ_{mb} [24].

The p_T differential cross section is modeled by a power law function, $A(p_0)^n/(p_T + p_0)^n$, for $p_T > 2$ GeV/c. In order to compare with the previous CDF K^0_S result [5, 25], p_0 is fixed at 1.3 GeV/c, and the results are shown in Tab. I. The data below $p_T \sim 2$ GeV/c cannot be described well by the power law function even if p_0 is allowed to float. For this region, the data are better described by an exponential function, $B \exp[-b \cdot p_T]$. The results of this fit are shown in Tab. II, and the slope b of Λ is consistent with previous measurements [12, 13]. The b values depend on the range of the fit but are about two, which corresponds to an average p_T of 1 GeV/c under the assumption that the fit can be extrapolated down to $p_T = 0$ GeV/c.

The plots on the right side of Fig. 2 show the ratio of the p_T differential cross sections for Ξ^- and Λ^0, and Ω^- and Λ^0. In the Ξ^-/Λ^0 ratio there is a rise at low p_T, and the ratio reaches a plateau at $p_T > 4$ GeV/c. It should be noted that the Λ^0 cross section also includes Λ^0 production from the decay of other hyperon states ($\Sigma^0 \to \Lambda^0\gamma$, $\Xi^\pm$, Ξ^0 and $\overline{\Xi}^0$). Due to the short Σ^0 lifetime, Λ^0 from Σ^0 decays cannot be separated from direct Λ^0 production. Simulations of cascade decays indicate that $\sim 50\%$ of Λ^0 from Ξ decays will satisfy our Λ^0 selection criteria, with the fraction of Λ^0 fairly independent of Ξ p_T. The ratio plots in Fig. 2 are fitted to a constant, and the value 0.17 ± 0.01 is obtained for Ξ^-/Λ^0 and 0.025 ± 0.002

TABLE II: The results of exponential function fits to the p_T differential cross sections shown in Fig. 2 for the p_T ranges given in the second row. The uncertainties shown do not include the MB cross section uncertainty [24]. The last line of the table gives the χ^2 per degree-of-freedom of the fit to data.

Parameter (units)	Λ^0	Λ^0	$\Xi^{\pm}$	$\Omega^{\pm}$
p_T range (GeV/c)	[1.2, 2.5]	[1.2, 4]	[1.5, 4]	[2, 4]
B (mb/GeV$^2c^3$)	4.68 ± 1.04	3.16 ± 0.35	0.16 ± 0.04	0.024 ± 0.011
b (GeV^{-1}c)	2.30 ± 0.12	2.10 ± 0.04	1.75 ± 0.08	1.80 ± 0.19
χ^2/dof	1.0/7	7.2/12	4.0/8	6.3/3

for Ω^-/Λ^0.

The plots in Fig. 2 clearly show that the cross sections depend on the number of strange quarks. However, the similarity of the n values in Tab. I, along with the measured value $n = 8.28 \pm 0.02$ for all charged particles [26], indicate that the slope of the p_T differential cross sections are similar in the high p_T region. This could be an indication of a universality in particle production as p_T increases [27]. This is in contrast to the low p_T region where the slope exhibits a strong particle type dependence [28].

Figure 3 shows the p_T differential cross sections for two charged-particle multiplicity regions, $N_{ch} < 10$ and $N_{ch} > 24$. $N_{ch} = 24$ (10) corresponds to $dN/d\eta \sim 16$ (7), corrected for the track reconstruction efficiency and unreconstructed tracks with $p_T < 0.3$ GeV/c [26]. Due to the low Ω^- sample statistics, distributions are only shown for Λ^0 and Ξ^-. We observe a correlation between high p_T particles and high multiplicity events. This is a general characteristic independent of the particle types.

In summary, the production properties of Λ^0, Ξ^-, and Ω^- hyperons reconstructed from minimum-bias events at $\sqrt{s} = 1.96$ TeV are studied. The inclusive invariant p_T differential cross sections are well modeled by a power law function above 2 GeV/c p_T. With fixed p_0, the fit parameter n decreases from 8.81 ± 0.08 (Λ^0) to 8.06 ± 0.34 (Ω^-). The low p_T regions are modeled by an exponential function. The exponential slope, b, decreases by $\sim 15\%$ from Λ^0 to Ω^-. The cross section ratios Ξ^-/Λ^0 and Ω^-/Λ^0 are presented as a function of p_T. Although the ratios exhibit a strong dependence on the number of strange quarks, the n values of the hyperons, K^0_S and all charged particles are within $\sim 10\%$ of each other. This

could be an indication that the production process which determines the p_T of these particles depends little on the particle type as p_T increases. We also find the hyperon p_T differential cross sections fall off faster with p_T for low multiplicity events than for high multiplicity events.

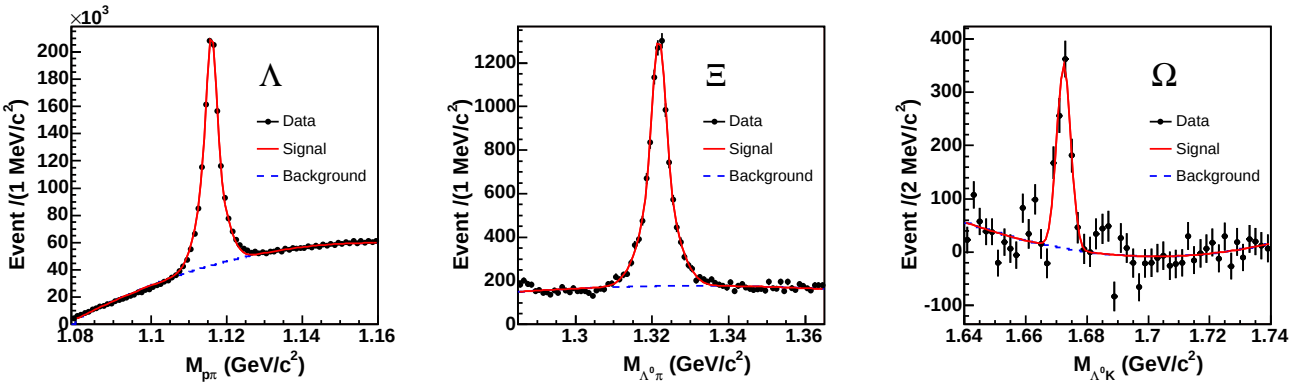

FIG. 1: Reconstructed invariant mass distributions for $M_{p\pi}$ (left), $M_{\Lambda^0\pi}$ (center), and $M_{\Lambda^0 K}$ (right). The background has been subtracted from the $M_{\Lambda^0 K}$ distribution. The solid lines are fitted curves, a third-degree polynomial for the background and either a double ($M_{p\pi}$ and $M_{\Lambda^0\pi}$) or single ($M_{\Lambda^0 K}$) Gaussian function to model the peak. The widths reflect the tracking resolution and are consistent with the widths from MC simulation.

We thank the Fermilab staff and the technical staffs of the participating institutions for their vital contributions. This work was supported by the U.S. Department of Energy and National Science Foundation; the Italian Istituto Nazionale di Fisica Nucleare; the Ministry of Education, Culture, Sports, Science and Technology of Japan; the Natural Sciences and Engineering Research Council of Canada; the National Science Council of the Republic of China; the Swiss National Science Foundation; the A.P. Sloan Foundation; the Bundesministerium für Bildung und Forschung, Germany; the World Class University Program, the National Research Foundation of Korea; the Science and Technology Facilities Council and the Royal Society, UK; the Institut National de Physique Nucleaire et Physique des Particules/CNRS; the Russian Foundation for Basic Research; the Ministerio de Ciencia e Innovación, and Programa Consolider-Ingenio 2010, Spain; the Slovak R&D Agency; and the Academy of Finland.

[1] G. D. Rochester and C. C. Butler, Nature **160**, 855 (1947).

[2] M. Athoff *et al.* (TASSO Collaboration), Z. Phys. **C 27**, 27 (1985); W. Braunschweig *et al.* (TASSO Collaboration), Z. Phys. **C 47**, 167 (1990); H. Aihara *et al.* (TPC Collaboration), Phys. Rev. Lett. **54**, 274 (1985); D. De La Vaissiere *et al.* (MARK-II Collaboration), Phys. Rev. Lett. **54**, 2071 (1985); H. Schellman *et al.* (MARK-II Collaboration), Phys. Rev. **D 31**, 3013 (1985); M. Derrick *et al.* (HRS Collaboration), Phys. Rev. **D 35**, 2639 (1987); W. Braunschweig *et al.* (TASSO Collaboration), Z. Phys. **C 45**, 209 (1989); H. Behrend *et al.* (CELLO Collaboration), Z. Phys. **C 46**, 397 (1990); D. Buskulic *et al.* (ALEPH Collaboration), Z. Phys. **C 64**, 361 (1994); P. Abreu *et al.* (DELPHI Collaboration), Z. Phys. **C 65**, 587 (1995); M. Acciarri *et al.* (L3 Collaboration), Phys. Lett. **B 328**, 223 (1994); P. Acton *et al.* (OPAL Collaboration), Phys. Lett. **B 291**, 503 (1992).

[3] M. Derrick *et al.* (ZEUS Collaboration), Z. Phys. **C 68**, 29 (1995); J. Breitweg *et al.*, Eur. Phys. J. **C 2**, 77, (1998); S. Akid *et al.* (H1 Collaboration), Nucl. Phys. **B 480**, 3 (1996); C. Adloff *et al.* (H1 Collaboration), Z. Phys. **C 76**, 213 (1997).

[4] R. Ansoge *et al.* (UA5 Collaboration), Z. Phys. **C 41**, 179 (1988); R. Ansoge *et al.* (UA5 Collaboration), Nucl. Phys. **B 328**, 36 (1989); G. Bocquet *et al.* (UA1 Collaboration), Phys. Lett. **B 366**, 441 (1996).

[5] D. Acosta *et al.* (CDF Collaboration), Phys. Rev. **D 72**, 052001 (2005).

[6] B. I. Abelev *et al.* (STAR Collaboration), Phys. Rev. **C 75**, 064901, (2007).

[7] P. Koch, B. Mueller and J. Rafelski, Phys. Rep. **142**, 321 (1986).

[8] M. Bourquin *et al.* (Bristol-Geneva-Heidelberg-Orsay-Rutherford-Strasbourg Collaboration), Z. Phys. C **5**, 275 (1980).

[9] T. Akesson *et al.* (Axial Field Spectrometer Collaboration), Nucl. Phys. B **246**, 1 (1984).

[10] B. I. Abelev *et al.* (STAR Collaboration), Phys. Rev. C **75**, 064901 (2007).

[11] G. J. Alner *et al.* (UA5 Collaboration), Phys. Lett. B **151**, 309 (1985).

[12] S. Banerjee *et al.* (E735 Collaboration), Phys. Rev. Lett. **62**, 12 (1989).

[13] T. Alexopoulos *et al.* (E735 Collaboration), Phys. Rev. D **46**, 2773 (1992).

[14] A. Abulencia *et al.* (CDF Collaboration), J. Phys. G **34**, 2457 (2007).

[15] A. Sill *et al.*, Nucl. Instrum. Methods A **447**, 1 (2000).

[16] In the CDF coordinate system, θ and ϕ are the polar and azimuthal angles of a track, respectively, defined with respect to the proton beam direction, z. The pseudorapidity η is defined as $-\ln[\tan(\theta/2)]$. The transverse-momentum of a particle is $p_T = p\sin\theta$. The rapidity is defined as $y = 0.5\ln[(E+p_z)/(E-p_z)]$, where E and p_z are the energy and longitudinal momentum of the particles associated with the track.

[17] A. Affolder *et al.* (CDF Collaboration), Nucl. Instrum. Methods A **526**, 249 (2004).

[18] D. Acosta *et al.*, Nucl. Instrum. Methods A **494**, 57 (2002).

[19] The impact parameter d_0 is the distance of closest approach of a track and the primary vertex in the $r-\phi$ plane.

[20] The number of p_T intervals for data is dictated by statistics such that the fits to the invariant mass distributions are stable. In the acceptance calculation, the number of p_T points is chosen such that a smooth acceptance curve as a function of p_T can be obtained. The statistical uncertainties of the acceptance values are less than a few percent.

[21] C. Amsler *et al.* (Particle Data Group), Phys. Lett. B **667**, 1 (2008).

[22] T. Sjöstrand, P. Eden, C. Friberg, L. Lonnblad, G. Miu, S. Mrenna, and E. Norrbin, Comput. Phys. Commun. **135**, 238 (2001).

[23] R. Brun, R. Hagelberg, M. Hansroul, and J. C. Lassalle, version 3.15, CERN-DD-78-2-REV.

[24] The total cross section corresponding to the minimum-bias trigger is estimated to be 45 ± 8 mb. The elastic (17 ± 4 mb [21]), single diffractive SD (12 mb), and half of the double diffractive DD (4 mb) cross sections are subtracted from the total $p\overline{p}$ cross section (78 ± 6 mb [21]) to give this estimate. The SD and DD cross sections are estimated using PYTHIA. A simulation study shows that the minimum-bias trigger is sensitive to $\sim 100\%$ of inelastic events which are not SD or DD and $\sim 50\%$ of DD events. A 100% uncertainty is assigned to the DD contribution.

[25] F. Abe *et al.* (CDF Collaboration), Phys. Rev. D **40**, 3791 (1989).

[26] F. Abe *et al.* (CDF Collaboration), Phys. Rev. Lett. **41**, 1819 (1988). This is at $\sqrt{s} = 1800$ GeV.

[27] A manuscript on a high statistics measurement of K^0_S, $K^{*\pm}(892)$ and $\phi^0(1020)$ production properties is in preparation.

[28] A.M. Rossi *et al.*, Nucl. Phys. **B 84**, 269 (1975); R.E. Ansorge *et al.* (UA5 Collaboration), Phys. Lett. B **199**, 311 (1987); G.J. Alner *et al.* (UA5 Collaboration), Nucl. Phys. **B 258**, 505 (1985); S. Banerjee *et al.* (E735 Collaboration), Phys. Rev. Lett. **64**, 991 (1990).

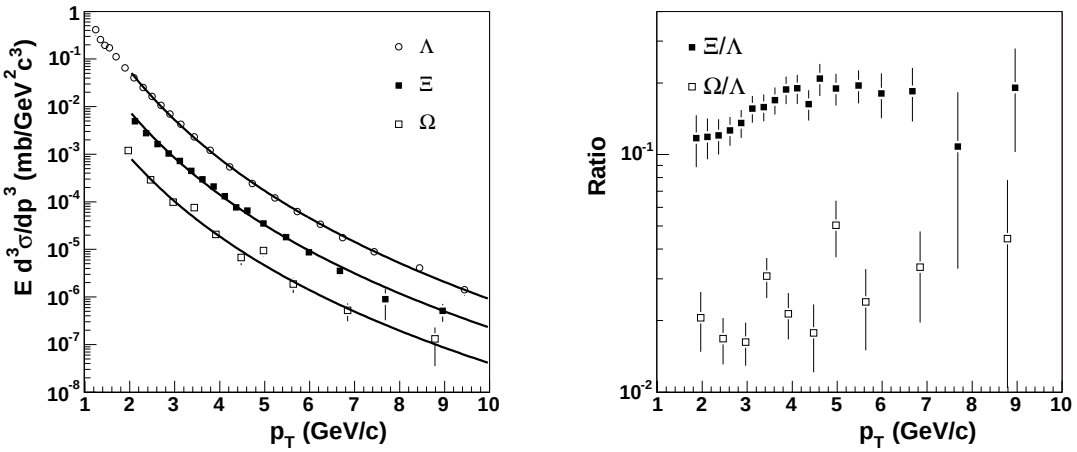

FIG. 2: The p_T differential cross sections for Λ^0, Ξ^-, and Ω^- within $|\eta| < 1$ (left). The solid curves are from fits to a power law function, with the fitted parameters given in Tab. I. The ratios of Ξ^-/Λ^0 and Ω^-/Λ^0 as a function of p_T (right).

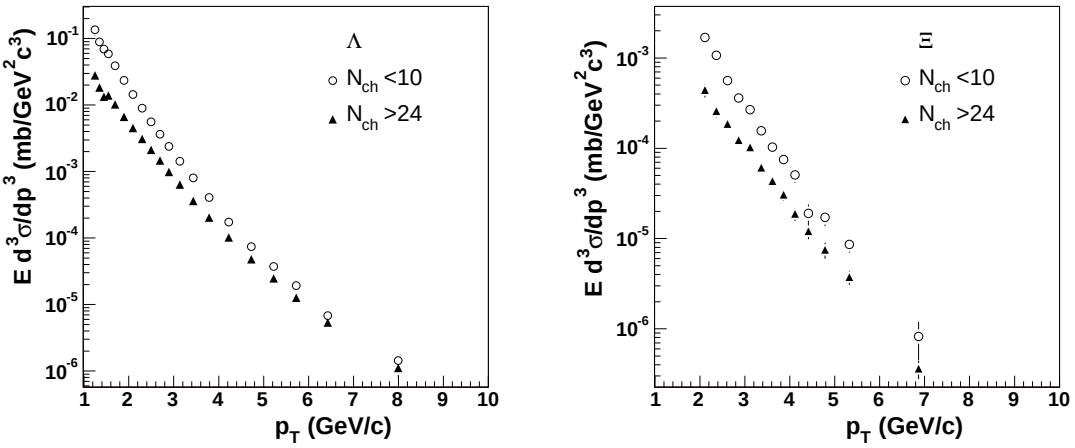

FIG. 3: The p_T differential cross sections for two charged-particle multiplicity regions, $N_{ch} < 10$ and $N_{ch} > 24$. Distributions for Λ^0 are shown on the left while distributions for Ξ^- are shown on the right.